Effects of neural stem cell and olfactory ensheathing cell co-transplants on tissue remodelling after transient focal cerebral ischemia in the adult rat

Ingrid Lovise Augestad [1§], Axel Karl Gottfrid Nyman[2§], Alex Ignatius Costa[3], Susan Carol Barnett[4], Axel Sandvig[1,5], Asta Kristine Håberg[1, 6, *], and Ioanna Sandvig[1]

[1] Department of Neuroscience, Faculty of Medicine, NTNU, Norwegian University of Science and Technology, Trondheim, Norway; ingrid.augestad@ntnu.no
[2] Department of Circulation and Medical Imaging, Faculty of Medicine, NTNU, Norwegian University of Science and Technology, Trondheim, Norway; axel.nyman@ntnu.no
[3] Department of Biotechnology, Faculty of Natural Sciences and Technology, NTNU, Norwegian University of Science and Technology, Trondheim, Norway
[4] Institute of Infection, Immunity and Inflammation, University of Glasgow, Scotland
[5] Division of Pharmacology and Clinical Neurosciences, Department of Neurosurgery and Clinical Neurophysiology, Umeå University, Umeå, Sweden
[6] Department of Radiology and Nuclear Medicine, St. Olavs, Trondheim University Hospital, Trondheim, Norway

[§] These authors have contributed equally.

***** Correspondence: asta.haberg@ntnu.no; Tel.: +4773551352

Acknowledgments and conflict of interest

ILA, AKH, AS, and IS would like to acknowledge funding by the Liaison Committee between the Central Norway Regional Health Authority and the Norwegian University of Science and Technology - Samarbeidsorganet HMN-NTNU. Additionally, IS and AS acknowledge funding by the Norwegian Financial Mechanism 2009–2014 and the Czech Ministry of Education, Youth and Sports under Project Contract no. MSMT-28477/2014, project 7F14057. The authors would like to thank Dr. Marius Widerøe for technical assistance with setting up the MR scanning parameters. Many thanks to Professors Berit Strand and Michel Modo for useful discussions. The authors have no conflict of interest to declare.

Abstract

Effective transplant-mediated repair of ischemic brain lesions entails extensive tissue remodeling, especially in the ischemic core. Neural stem cells (NSCs) are promising reparative candidates for stroke induced lesions, however, their survival and integration with the host-tissue post-transplantation is poor. In this study, we address this challenge by testing whether co-grafting of NSCs with olfactory ensheathing cells (OECs), a special type of glia with proven neuroprotective, immunomodulatory, and angiogenic effects, can promote graft survival and host tissue remodelling. Transient focal cerebral ischemia was induced in adult rats by a sixty-minute middle cerebral artery occlusion (MCAo) followed by reperfusion. Ischemic lesions were verified by neurological testing and magnetic resonance imaging (MRI). Transplantation into the globus pallidus of NSCs alone or in combination with OECs was performed at two weeks post-MCAo, followed by histological analyses at three weeks post-transplantation. We found evidence of extensive vascular remodelling in the ischemic core as well as evidence of NSC motility away from the graft and into the infarct border in severely lesioned animals co-grafted with OECs. These findings support a possible role of OECs as part of an *in situ* tissue engineering paradigm for transplant mediated repair of ischemic brain lesions.

Keywords: stroke; tissue engineering; vascular remodeling; CNS regeneration

Introduction

Ischemic stroke is one of the leading causes of disability-adjusted life-years (DALYs) worldwide, i.e. the number of life-years lost due to premature death and years lived with disability adjusted for severity, and accounts for 80-85% of all stroke incidents [1]. Ischemic stroke is caused by embolic or thrombotic obstruction of blood supply to the brain. An ischemic event triggers a complex molecular cascade including impaired cellular energy metabolism, cell depolarization, excitotoxicity, and disruption of the blood–brain barrier [1]. Depending on the duration of the ischemic event, these pathophysiological changes can lead to extensive neuronal and glial cell injury and/or death, and axonal loss or demyelination, resulting in severe functional deficits [2]. The brain tissue where blood flow is most severely reduced comprises the ischemic core and is characterized by rapid pannecrosis. The ischemic core is surrounded by the ischemic penumbra, which represents salvageable tissue but only within a limited time frame [3]. At present, the only proven medical intervention for the treatment of acute stroke involves thrombolysis with tissue plasminogen activator and/or endovascular mechanical thrombectomy, and aims to dissolve the embolic or thrombotic obstruction. However, tissue plasminogen activator can only be administered within a maximum of 4.5 hours (h) after the onset of stroke [4], which effectively excludes more than 85% of stroke patients from this treatment. Cell replacement therapy in the sub-acute or chronic stage offers the option of extending the narrow therapeutic window while addressing a key constituent of stroke pathophysiology, namely the cell loss caused by ischemia. In this context, a number of studies have demonstrated the potential of stem cell treatment in promoting tissue remodeling in animal models of ischemic stroke injury [5-9].

Neural stem cells (NSCs) are self-renewing multipotent progenitors that can differentiate into both neurons and glia, a property that renders them highly relevant for central nervous

system (CNS) repair [10, 11]. However, NSC survival post-engraftment is generally poor, especially in the ischemic core of large lesions [12]. Olfactory ensheathing cells (OECs), the glia surrounding the primary olfactory neurons throughout their trajectory from the olfactory mucosa to the olfactory bulb glomeruli, possess several attributes that make them particularly interesting in the repair of CNS lesions [13]. OECs secrete a host of growth factors, including vascular endothelial growth factor (VEGF), brain-derived neurotrophic factor (BDNF), glial cell line-derived neurotrophic factor (GDNF), and nerve growth factor (NGF), all of which are important for neural, glial and endothelial cell function as demonstrated in a number of experimental studies [14-19]. Furthermore, compared to Schwann cells, OECs induce less astrocytic response in *in vitro* confrontation assays [20] as well as following transplantation into adult CNS white matter [21]. We have previously demonstrated the capacity of OECs to promote tissue remodelling, including axonal sparing and plasticity, neovascularization and remyelination after induced central axotomy [19], while a recent clinical report suggests that OECs combined with Schwann cell transplants can promote functional regeneration of supraspinal connections after spinal cord injury [22]. Furthermore, growing evidence from experimental studies suggests that apart from being neuroprotective to injured neurons, OECs interact with astrocytic processes to form pathways that can help bridge the lesion cavity by providing a microenvironment permissive to axonal growth, a mechanism described as the 'pathway hypothesis' by providing structural, as well as biochemical support [23, 24]. Taken together, the above attributes suggest that if OECs are co-engrafted with NSCs, they may enhance the viability and function of the NSC graft and synergistically act to achieve *in situ* tissue engineering after a focal ischemic lesion.

In this study, we used the middle cerebral artery occlusion (MCAo) model to induce transient focal cerebral ischemia in adult rats and investigated whether NSC and OEC co-transplants engrafted in the basal ganglia can promote tissue remodelling.

Materials and Methods

Cell culture and labelling

OECs from neonatal rats were purified as previously described [20]. Briefly, the olfactory bulbs of 4-5 P7 *Sprague Dawley* rats were harvested and finely chopped, then enzymatically digested in L-15 (Leibovitz) medium (Sigma), and triturated through a 26 gauge needle. Dissociated cells were incubated in a cocktail of O4 (IgM at 1:4) and anti-galactocerebroside (IgG3 at 1:2) primary antibodies (Clonetech), followed by their fluorochrome conjugated class specific secondary antibodies (Life Technologies). Further, dissociated cells were rinsed and then incubated in goat anti-mouse IgM phycoerythrin and goat anti-mouse IgG3 fluorescein secondary antibodies (1:100, Southern Biotech, Cambridge, UK). OECs were purified by fluorescence activated cell sorting (FACS) (Becton Dickenson, Oxfordshire, UK) by selecting for galactocerebroside-negative and O4-positive cells. Subsequently, OECs were cultured in Dulbecco's Modified Eagle's Medium (DMEM) GlutaMAX® (Sigma-Aldrich Company Ltd., Dorset, UK) with 1.25% gentamicin (Sigma), and 5% FBS (Autogen Bioclear, Wiltshire, UK) on 13 μg/ml poly-L-lysine- (PLL) (Sigma) coated 25cm2 flasks (Sigma). The cultures were supplemented with 500 ng/ml fibroblast growth factor 2 (FGF2) (Peprotech, London, UK) 50 ng/ml heregulin (hrgβ1) (R&D Systems Europe Ltd, Abingdon, UK), and 10-6 M forskolin (Sigma). Finally, OECs were passaged at confluence. Purity of the OECs populations was assessed by p75NTR specific labelling and was always at 98-100%. In order to investigate the

distribution of OECs at the graft site, OECs were engineered to express enhanced green fluorescent protein (eGFP, Clontech, Living Colors). Shortly after purification, subconfluent cultures of OEC were infected overnight with transient supernatant taken from eGFP transfected phoenix cells, as previously described [17]. Transfection efficacy was determined by fluorescence microscopy of retrovirally labelled OEC cultures and was at 70-80%.

H9 (human embryonic) NSCs (GIBCO®, Invitrogen, Life Technologies, Carlsbad, CA, USA) were cultured in 75 cm2 flasks coated with CELLStart™, a xeno-free cell culture substrate (Invitrogen, life Life Technologies). The cultures were fed with Complete StemPro® serum-free NSC medium (Invitrogen, life Technologies), kept in a standard humidified air incubator with 5% CO2, at 37°C, and passaged twice at about 90% confluence before transplantation. Early passage (P3) primary NSCs at 90% confluence were stained with PKH26 cell linker kit (Sigma) immediately prior to *in vitro* co-culture studies or transplantation, as appropriate, according to the manufacturer's instructions.

To determine optimal seeding density (i.e. number of cells/cm^2) for NSC-OEC co-cultures, a series of co-culture assays were performed at relative proportions of NSC:OEC of 70:30, 50:50, and 30:70, in the presence of OEC and/or NSC culture media.

Animal procedures

All animal procedures were approved by the Norwegian ethics committee and were conducted in accordance with the relevant national, regional and site guidelines. Male *Sprague Dawley* rats (9 weeks old; 225-280 g, at start) were purchased from Scanbur AS. Cages were kept in a 12:12 h light/dark cycle, and animals had ad libitum access to food pellets and water.

Middle cerebral artery occlusion (MCAo)

The animals were randomly assigned into two groups for surgery; (i) sham MCAo (n=5) and (ii) MCAo (n=30). Right middle cerebral artery occlusion (MCAo) was performed under anaesthesia with Hypnorm/Dormicum (Fluanizon/Fentanyl/Midazolam) using the intraluminal filament technique [25, 26]. The animals remained anaesthetized for 60 min when the monofilament was withdrawn to allow for reperfusion. Xylocaine spray 10mg/ml (Astra Zeneca) was topically applied to the incision before suturing and returning the animals to their cages, where they were kept under observation and allowed to wake up. Post-operative food intake was supported by administration of pellets soaked in Nutridrink (Nutricia).

Verification of stroke-induced brain lesions

Verification of stroke lesions included neurological scoring using the Bederson scale in combination with T2-weighted magnetic resonance imaging (MRI) obtained at 1 week post-injury (wpi). For MRI, the animals were placed prone on a dedicated water-heated bed within a 7T small animal scanner (Biospec 70/20 AS, Bruker Biospin MRI, Ettlingen, Germany) with water-cooled gradients (BGA-12S, 660 mT/m). An 86 mm volume resonator was used for radiofrequency (RF) transmission and a phased array rat head surface coil was used for RF reception. T2-weighted images were obtained under isoflurane anaesthesia (2% isoflurane in 30% O2/70% N2) using a rapid acquisition with relaxation enhancement (RARE) sequence with effective echo time (TE) = 30 ms; repetition time (TR) = 3700 ms; number of averages (NA) = 8; Rare Factor = 8; field of view (FOV) = 20.4 x 16 mm2; acquisition matrix 204 x 160; 32 coronal slices à 0.5 mm; scan time = 4m 56s. The T2-weighted images were scored by a blinded observer with experience in evaluating rat brain MR images. Inclusion criteria for allocation into treatment groups were defined as: animals with observed hyperintensities in the ipsilateral striatum, or ipsilateral

cortex (S1 or S2), or ipsilateral thalamus, which also matched with a neurological score of >1 on the Bederson scale at 1wpi. Using these criteria, 17 (57 %) animals were included for treatment randomization.

Intracranial cell transplantation

Based on post-operative neurological assessment and MRI data obtained at 1w after MCAo, animals with confirmed ischemic injury were randomly assigned into three groups for intrastriatal cell transplantation at 2wpi, as follows: 1) untreated controls (n=4); injection of 3 µl saline, 2) NCS group (n=6); injection of 3 µl of 3×10^5 NSC suspension, and 3) NSC and OEC group (n=7); injection of 3×10^5 NSC-OEC suspension at a proportion of 50:50. For transplantation, the animals were placed in a rat head stereotactic frame (Kopf Instruments) under 1.5-2% isoflurane anaesthesia. Local anaesthesia was administered subcutaneously, before exposing the skull by midline incision. Injection coordinates were determined with reference to the Bregma, using the Paxinos Watson rat brain atlas (Elsevier) at AP -1.3, L -3.5, V -7.0, representing the ipsilesional globus pallidus, consistent with a previous study [7]. After making a burr hole, a total volume of 3 µl of cell suspension (or saline) was injected at a rate of 1 µl/min using a Hamilton syringe attached to an UltraMicroPump (UMP3) with SYS-Micro4 Controller (World Precision Instruments Ltd, Hitchin, Herdfordshire, UK). To avoid reflux, at the end of the injection, the needle was left inside the skull for another 2 min before being slowly withdrawn. The burr hole was subsequently sealed with sterile bee's wax and the incision sutured before the animals were returned to their cages. Immunosuppression was not considered necessary due to the relatively low immunogenicity of NSCs [27] and the fact that the OECs were homologously derived.

4.2.4. Cylinder rearing test

The animals' locomotor asymmetry was evaluated using the cylinder rearing test. Briefly, at 10 and 11 days post-injury (dpi), 4 days post-transplantation (dpx), and 21 dpx, animals were placed in a glass cylinder (67 cm tall, 15 cm diameter) and video recorded for five minutes (21). Three mirrors were arranged so that contacts between the forepaws and the cylinder wall could be monitored at all times. The videos were subsequently reviewed frame-by-frame separately by two observers blinded to experimental group assignment and the number of contacts between the forepaw and the cylinder wall were counted and registered as left (NL) or right (NR). Only contacts involving all digital pads and the palmar pads were registered. A normalized forepaw preference ratio (FP) was then calculated for each limb in each animal: $\frac{NL}{total} \times 100 = Left\ paw\ ratio$, or $\frac{NR}{total} \times 100 = Right\ paw\ ratio$.

Intracardial perfusion and tissue collection

At 3 wpx, the animals were sedated with 3.5% isoflurane, given a lethal injection of Pentobarbital (1mL/kg), and exsanguinated by means of intracardial perfusion with 50 mL chilled phosphate buffered saline (PBS) solution followed by 50 ml 4% paraformaldehyde. The whole brain was then removed and post-fixed in 4% paraformaldehyde at 4°C overnight and cryoprotected by immersion in 30% sucrose for 2-3 days at 4°C before being embedded in OCT compound (BDH), frozen in liquid nitrogen and stored at -80°C.

Volumetry

Lesion volumes were calculated for each rat based on differences in hyperintensities in the T2 MR images using OsiriX (Pixmeo, Geneva, Switzerland) and an Intuos Creative Pen Tablet (Wacom Company, Ltd). The areas in each slice of the T2 scan from each rat that showed a hyperintense area relative to the contralateral hemisphere, were outlined using an Intuos Pen, before computing the ROI volume in OsiriX (Figure 1). Classification of lesion

severity based on lesion volume computations was as follows: (i) small lesion: volume <30 µL; (ii) moderate lesion: volume 30 µL – 80 µL; and severe lesion: volume >80 µL.

Immunohistochemical analyses of brain tissue

50 µm-thick sections of post-mortem tissue were serially collected using a Leica CM3050S cryostat and placed on Superfrost® Plus glass slides (Fisher Scientific). Immunohistochemistry included the following steps: immersion in blocking solution consisting of 5% goat serum and 0.3% Triton X-100 in phosphate buffered saline (PBS) for 1 h at room temperature (RT), followed by incubation with primary antibodies in a solution of 1% goat serum and 0.1% Triton-X in PBS at 4°C overnight. Primary antibodies included: anti-nestin rabbit polyclonal antibody (dilution 1:1000), anti-CD68 mouse monoclonal antibody (1:1000); anti-GFP rabbit polyclonal antibody (1:500), anti-collagen IV rabbit polyclonal antibody (1:300), and mouse monoclonal anti-human nuclei (HuNu) (Merck Millipore). The sections were then washed three times in PBS before incubation with their class-specific secondary antibodies AlexaFluor 568 and AlexaFluor 488 (Invitrogen, Life Technologies) with Hoechst (1:5000) for 3h at RT. The sections were subsequently washed in PBS, coverslipped with Fluorsave (Merck Millipore), and imaged on an Olympus Scan R or Zeiss Axiovert A1 fluorescent microscope. Images were post-processed in Image J (U. S. National Institutes of Health, Bethesda, USA) for manual and automated cell counts.

Statistical analyses

Statistical differences between groups were determined by two-way ANOVA (not repeated measures), paired t-tests using a significance level of 95%, and Fisher's exact test using Prism 7 for Mac OS X (GraphPad Software, Inc, San Diego, CA, USA). Post hoc power for paired t-tests was analysed using G*Power (Version 3.1.9.2).

Results

Verification and evaluation of severity of stroke-induced lesions

T2-weighted magnetic resonance imaging (MRI) at one week (w) post-injury (wpi), associated with a neurological score of >1 on the Bederson scale, verified the presence of MCAo-induced brain lesions and subsequent inclusion of the animals in the study. The T2-weighted MR images revealed stroke-induced lesions in the form of hyperintensities observed primarily in the ipsilesional striatum, and/or frontal, parietal, and temporal cortex, but also in varying degrees in the thalamus, hypothalamus, cervicomedullary junction and substantia nigra. As expected, the extent and degree of severity of the ischemic lesions induced by MCAo varied largely between rats (Figure 1A-D), thus mimicking the clinical situation [25, 28]. 3D reconstruction of the T2-weighted MR images (Figure 1E, F) and volumetric analyses further confirmed the variability in lesion severity, showing lesion volumes ranging from 7.6 µl – 130.5 µl. For each experimental group the median and range (in brackets) of the lesion volumes were as follows: The saline group had a median of 113.7 µl (96.8-130.5 µl); the NSC group had a median of 17.05 µl (10.7-20.0 µl); and the NSC-OEC group had a median of 54.25 µl (7.6-128.2 µl).

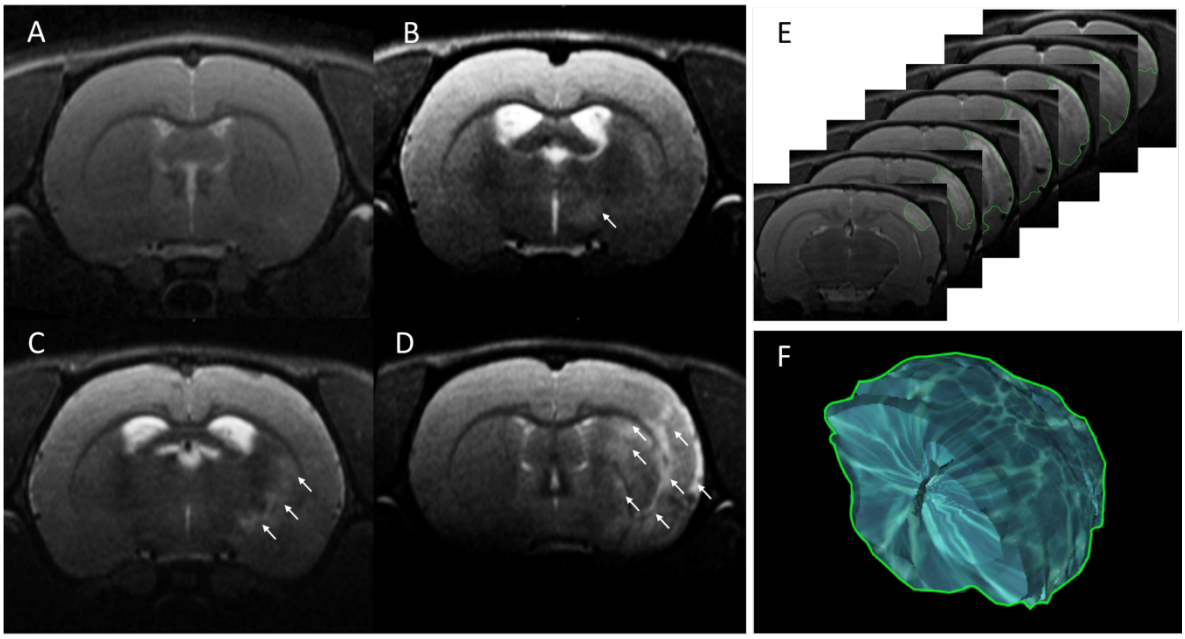

Figure 1) A-D. Representative images showing variability of lesion severity after MCAo as revealed by T2-weighted MRI. **A**. Sham animal. **B**. *Small lesion (volume <30 µl)*. **C**. Moderate lesion (volume 30 µl – 80 µl). **D**. Severe lesion (volume >80 µl). **E,F**. 3D reconstruction of MCAo-induced lesion volumes. The lesion volume for each rat was calculated by first outlining (green line) the hyperintense areas in each frame in the T2 images (E) and digitally constructing a 3D representation of the delineated lesion, as shown in F.

Formation of NSC-OEC networks in vitro

In vitro NSC and OEC co-culture assays revealed gradual formation of distinct OEC networks interlaced with NSCs (Figure 2). Optimal cell dispersal and survival were achieved with a proportion of 50:50 in NSC:OEC co-cultures fed with NSC media. Specifically, we found that this proportion resulted in homogeneous co-cultures in which both cells attached and displayed normal morphology, and where the cells covered the entire surface of the wells, without leaving any areas unpopulated and without any aggregation of either cell type in separate parts of the wells. Furthermore, these co-cultures yielded average cell counts of NSCs and OECs (expressed as mean ± standard deviation per unit area) of 34,532 ± 3,369/cm^2 and 19,021 ± 2,774/cm^2, respectively, at 48h post-seeding. This was comparable to the cell counts obtained from control cultures of each cell type separately at the same time point (NSCs: 38,119 ± 2,208/cm^2; OECs: 21,006 ± 4,595/cm^2).

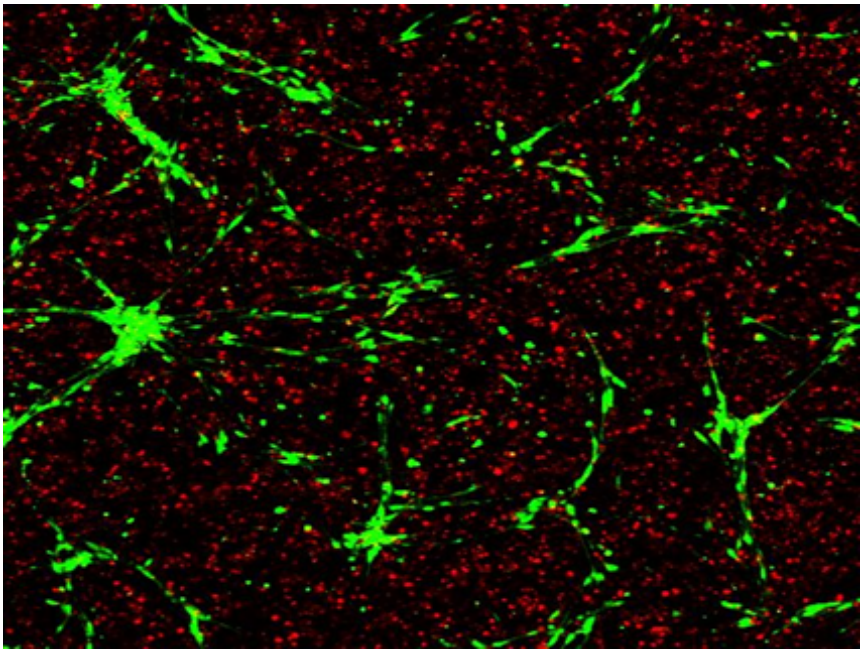

Figure 2) Formation of OEC networks in co-culture with NSCs. OECs (green; GFP) form distinct networks in co-culture with NSCs (red; PKH26); Scale bar: 10 µm.

Cell survival, motility and vascular remodelling post-transplantation

Contrary to the *in vitro* observations, we found little evidence of network formation in NSC-OEC grafts *in situ* at 3w post-transplantation (wpx) in the globus pallidus. Indeed, the two cell types appeared to form separate clusters, with OECs aggregating in the core of the graft and NSCs localised in the graft periphery (Figure 3 A-C). These observations were only made in animals with small ischemic lesions (lesion volume <30 µl), in which the basal ganglia were not severely affected.

As expected, NSC and NSC-OEC graft survival was better in animals with less severe lesions. Relatively good survival was observed for both cell types in the NSC-OEC grafts, albeit with NSC numbers on average 63% ± 14.4 higher than those of OECs. In these animals, both types of cells appeared to form tight clusters within the original graft location

with OECs always aggregating in the centre of the graft (Figure 3A-C). NSC-OEC grafts appeared much less clustered and more dispersed in animals with moderate and severe lesions (lesion volumes 30 µl – 80 µl, and >80 µl, respectively) (Figure 3 D-F), while overall NSC survival in these animals was significantly higher in the NSC-OEC group compared to NSC only (average number of NSCs/counting frame NSC/OEC group 87.6 ± 24.3, *versus* NSC group 31.3 ± 18.6; two-tailed $p < 0.05$; Fisher's exact test).

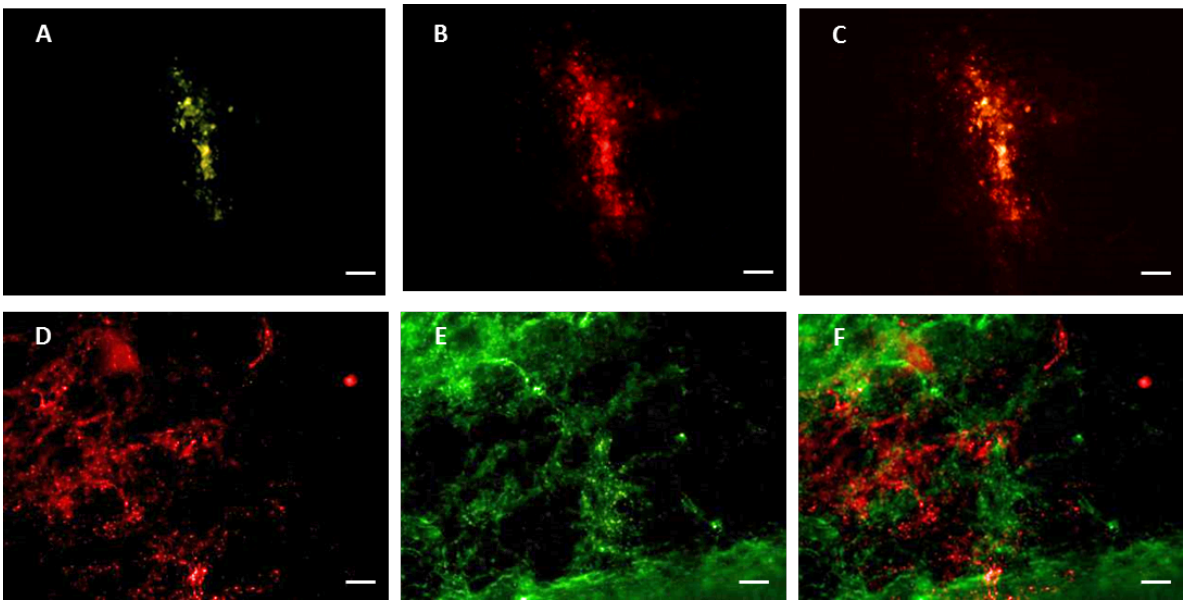

Figure 3) Representative images from animals with NSC-OEC co-grafts at 3w px. **A-C**. Clusters formed by the transplanted cells within the graft location in animals with small ischemic lesions; D-F. Motility of the engrafted cells and dispersal within the ispilesional striatum; A,D. OECs (green; GFP); B,E. NSCs (red; PKH26); C. Merge A,B; D. Merge D,E. Scale bar 50µm

In general, OEC survival was relatively poorer than that of NSCs, especially in animals with severe lesions, in which very few OECs (<1% of transplanted cells) were found. In co-grafted animals with moderate lesions, the average proportion of OECs per counting frame was 43.8 ± 11%. However, overall NSC survival in co-grafted animals with small and moderate lesions tended to be better than that of OECs ($p=0.054$; Fisher's exact test). It is not clear whether the relative absence of OECs from animals with severe lesions can be attributed to cell death or to possible migration away from the engraftment site post-

transplantation. However, we did not find any evidence of OEC migration regardless of lesion severity. Instead, we found notable NSC migration from the lesion core and into the infarct border in animals with moderate and severe lesions (Figure 4) as well as NSC migration from the graft site to the ipsilesional corpus callosum in animals with small lesions (Figure 5). Furthermore, immunostaining against nestin (Figure 5B) and anti-human nuclei antibody (Figure 5C) revealed larger numbers of NSCs than originally indicated by the PKH26 stain (Figure 5A), suggesting that PKH26 staining may underestimate the survival and/or migration of the engrafted NSCs post-transplantation. Interestingly, extensive vascular remodelling in the lesion core was observed in animals with severe lesions and NSC-OEC grafts at 3wpx (Figure 6).

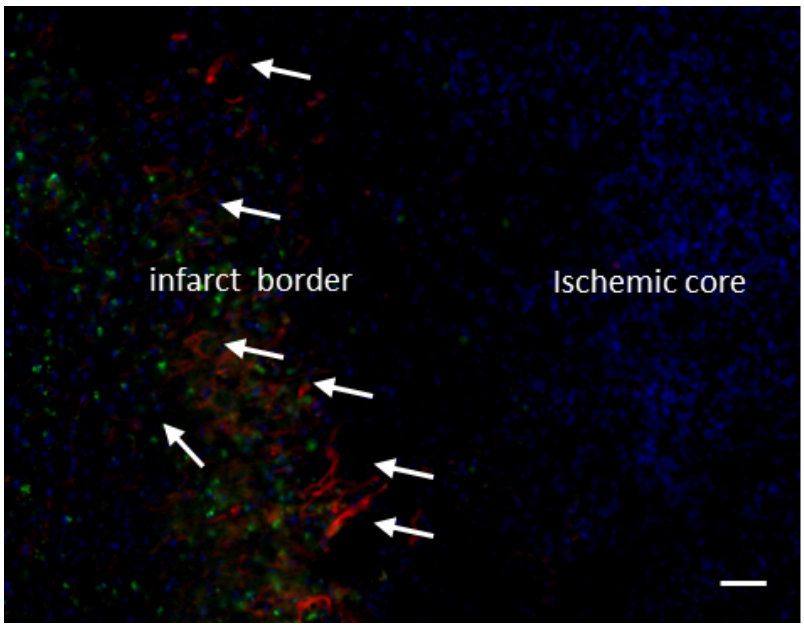

Figure 4) NSC migration into the infarct border in severely lesioned animals. Nestin-positive (red) NSCs with elongated neurite projections (arrows) can be observed along the border between the ischemic core and infarct border, integrating with the latter. Microglia (green; CD68) can also be observed in the infarct border (blue: Hoechst; Scale bar 50µm).

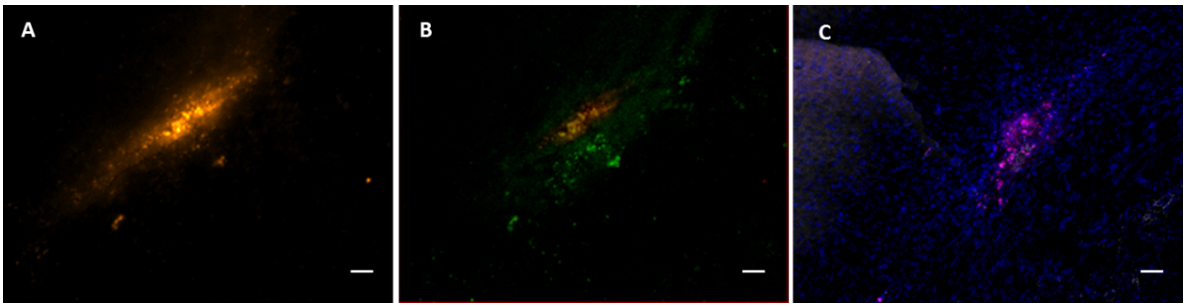

Figure 5) NSC migration along the ipsilesional corpus callosum in animals with small lesions. **A.** Migrating NSCs (PKH26: orange) along the corpus callosum; **B**. Immunostaining against nestin (green) reveals additional migrating NSCs to those indicated by PKH26 staining (orange). **C**. Anti-human nuclei antibody (purple: HuNu; blue: Hoechst). Scale bar 100µm.

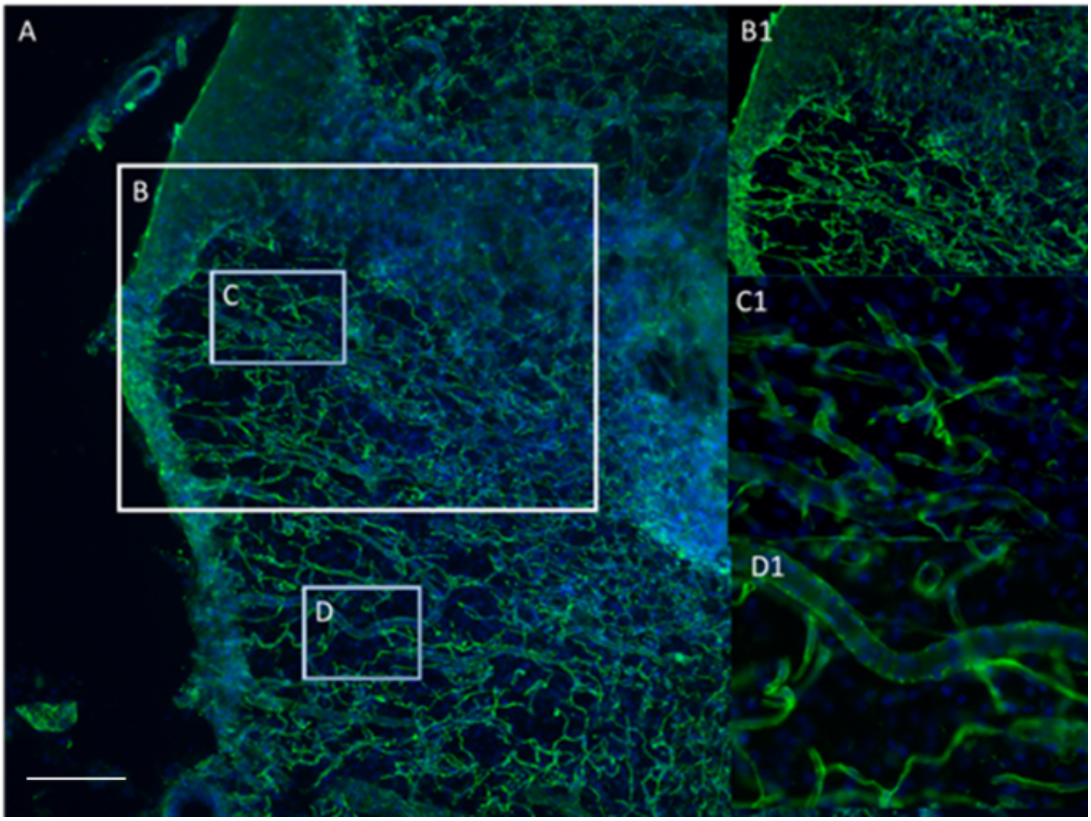

Figure 6) Vascular remodelling in the ischemic core of animals with severe lesions at 3 wpx. **A.** Evidence of extensive vascular remodelling as revealed by staining against Collagen IV (green) in the lesion core. Images B1-D1 on the right-hand column show higher magnification of corresponding areas boxed in **B-D**; (blue: Hoechst; scale bar 100µm).

Behavioural assessment

To assess forelimb functional asymmetries, the Cylinder Rearing Test was administered on day 10, 11, 16, and 28 post MCAo. A two-way repeated measures ANOVA showed no significant effects between left versus right forelimb preference, nor across timepoints ($F(2,14) = 3.631$). Paired t-tests showed no significant differences in right or left forelimb use within each group between day 10 and 28, i.e. before and after treatment ($p > 0.05$) (Figure 7). Post hoc power analysis of results from the paired t-tests yielded very low power ($\pi > 0.105$). This was expected due to the low number of animals in each group. However, there was an increased left forepaw preference in the saline treated control group, indicative of a trend towards improvement ($p = 0.295$, $\eta^2 = 0.744$).

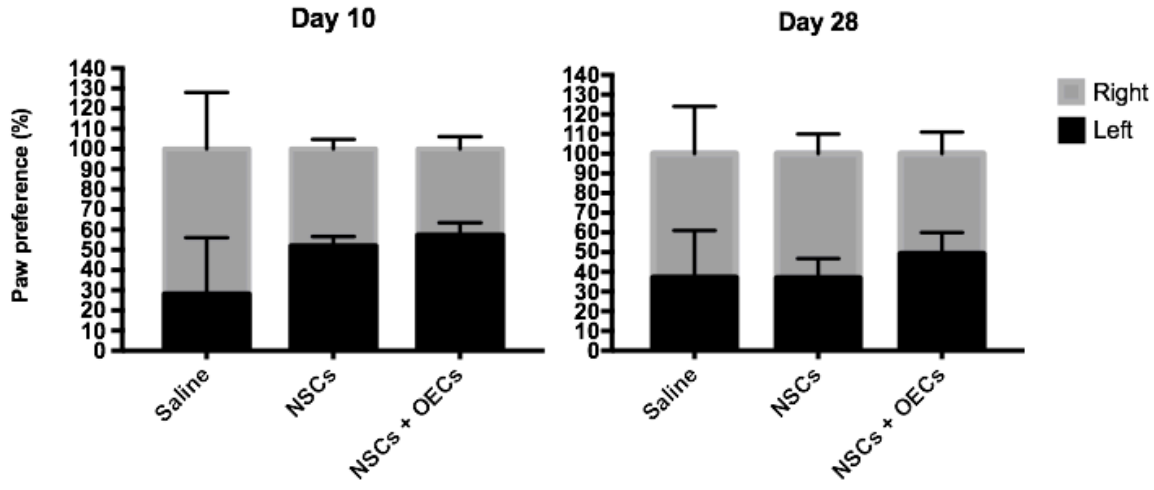

Figure 7) Results of lateral asymmetry test showing left forelimb versus right forelimb preference ratio on Day 10 post MCAo compared to Day 28. Data are presented as means ± standard error of the mean. Two-way ANOVA (not repeated measures) did not find any significant differences between left and right forelimb, or between time points.

Discussion

The formation of OEC networks in the *in vitro* co-culture with NSCs may constitute a predictor of OEC function post-transplantation. In particular, the self-organization of OECs

into relatively continuous elongated network-like structures in the culture seemed to partially recapitulate the natural orientation of these cells in their resident *milieu*, in which they align themselves with the axons of primary olfactory neurons [13]. Although we found no direct evidence of *in situ* OEC network formation post-transplantation, our results suggest a possible role of OECs in promoting tissue remodeling after stroke.

In particular, the evidence of an extensive vascular network in the lesion core of severely lesioned animals co-grafted with OECs could be attributed to potential stimulation of angiogenesis through local VEGF secretion from the transplanted OECs. Similarly, the overall NSC survival in animals that received NSC-OEC grafts suggests potential neuroprotective effects of the OECs on the transplanted NSCs, possibly through secretion of neurotrophic factors and cytokines. This is in accordance with previous findings, showing optimal effects of co-grafting NSCs with OECs in terms of promoting NSC survival and neuronal restoration after experimental traumatic brain injury and Parkinson's disease [29, 30] .

Furthermore, our findings might be in agreement with the 'pathway hypothesis' [31], according to which OECs may promote remodeling of disrupted neuronal pathways by acting as bridges which provide structural and/or biochemical support to regenerating axons or cell transplants [32, 33].

Specifically, we found evidence of NSC migration away from the graft, having moved from inside the lesion core and into the infarct border. Although we did not observe any OECs in the graft core or in the infarct border in these animals, the finding of a vascular network in

the lesion core, coupled to the presence of migrating nestin-positive NSCs in the infarct border, may constitute indirect proof of structural and biochemical support involving juxtacrine and/or paracrine effects attributable to the engrafted OECs. On the other hand, it would be difficult to justify the absence of OECs from these tissues as a result of potential cell death, given that the degree of vascular remodeling observed in the lesion core should also have supported the longer-term *in situ* survival of the engrafted OECs, in addition to that of the NSCs. Thus, one explanation could be that ability to detect the transplanted OECs based solely on the expression of the GFP reporter gene may be severely compromised, especially in animals with more severe ischemic lesions. This is because formation of the GFP fluorophore requires molecular oxygen to catalyze its posttranslational cyclization [34, 35], implying that this process may have been adversely affected by the hypoxic conditions prevailing in the lesion core post-transplantation, leading to gradual loss of GFP expression and, effectively, inability to retrieve it, even with the use of an anti-GFP antibody. An alternative explanation for the lack of observable OECs is that the cells may have ultimately migrated to other sites in the brain or entered the lateral ventricle, as previously reported for different intraparenchymal cell transplants after MCAo [36-38].

Another interesting perspective is how NSCs together with OECs may synergistically support *in situ* tissue remodeling after stroke injury. In a similar way in which NSC survival and integration with the host tissue may be promoted by the presence of OECs in the graft, as observed in animals with less severe lesions, the relatively good survival of the OECs in

the same animals may in turn be attributed to trophic support by the transplanted NSCs [39]. Notwithstanding the fact that reduced lesion severity will have provided a more favorable microenvironment in the host parenchyma, OEC survival post-transplantation in lesioned CNS tissue is generally expected to be poor [40]. Thus survival of OECs in these tissues may have been promoted by the presence of NSCs in the graft. Furthermore, given that a less severe lesion would also involve a less hypoxic host microenvironment, GFP expression in the transplanted OECs may not have been particularly affected, thus resulting in improved detectability. Overall, the difficulty of detecting surviving OECs based on GFP expression, might have been circumvented with the use of an OEC-specific antibody. However, in the absence of an unequivocal marker for OECs [40, 41], further immunostaining (i.e. in addition to anti-GFP antibody) for the purpose of identifying more surviving/migrating OECs was not relevant. In addition to the above, the tendency for aggregation of both NSCs and OECs in the original graft location, as opposed to any observable homing to other parts of the brain, could be explained by lower host tissue inflammation. Especially with regard to NSC transplants, their recruitment to affected parts of the brain is mediated by an increase in chemokine and cytokine production in response to the ischemic lesion [42]. Clearly, this effect can be expected to be less pronounced in smaller lesions.

Still, we found evidence of callosal migration in the form of NSC clusters aligned with the ipsilesional corpus callosum in animals with less severe lesions. Cross-callosal, transhemispheric migration has previously been reported, especially for bone-marrow

stromal cells. However, in those cases the stem cells were originally transplanted in the contralesional hemisphere after stroke induced injury [6, 43]. Furthermore, after ischemic lesion, intracortically transplanted NSCs have been shown to migrate away from the initial graft location and to align themselves with the corpus callosum [44]. These and other studies suggest that NSCs are able to migrate to parts of the brain remote from the original graft locations along white matter tracts. Notwithstanding the possibility that the observed NSCs aligned with the ipsilesional corpus callosum might be derived from a residual population at the dorsal end of the injection tract as a result of needle withdrawal post-injection, the absence of a visible needle tract in the tissue and the fact that the NSCs are also localized in sections anterior to the transplantation site, suggest that their presence in the corpus callosum may be the result of migration away from the globus pallidus, i.e. the transplantation site. Considering the relatively small lesion severity, NSC migration along existing white matter tracts, irrespective of any synergistic effects mediated by OECs should be possible.

The cylinder rearing test revealed no significant differences in the use of the contralesional (left) forepaw over time in either of the treatment groups, but indicated a trend towards improvement in the saline treated control group, which may be consistent with spontaneous functional recovery [45, 46]. The lack of improvement in forepaw preference after NSC or NSC-OEC transplantation is not surprising, considering that any functional benefits as a result of the treatment would be marginal, and thereby difficult to evaluate at 3wpx.

Furthermore, small group sizes, as here, are sensitive to type II errors, especially when considering both limb, group and time in the same analysis as in this study.

Moreover, systematic bias due to individual differences between rats' preferred forelimb use cannot be excluded [47, 48]. Thus, although the cylinder test may be useful for verifying stroke-induced functional deficits, its value in the assessment of gain of function in the present study may be limited.

Finally, a relevant point in the above discussion is the extent to which the choice of experimental model, i.e. 60-minute MCAo, may have impacted our findings. This specific model is well-characterized in the literature and has been used in a number of experimental studies of transient focal cerebral ischemia, including studies investigating intrastriatal stem cell transplantation [7, 49-52]. However, one challenge associated with the MCAo model is that it is known to result in lesions of variable severity [7, 52-54]. While this *per se* may be considered positive in terms of the extent to which the MCAo model can recapitulate the variability observed in stroke patients, such differences in lesion severity, coupled to the strict criteria which were applied for the inclusion of lesioned animals in the study, did result in relatively small group sizes. Another relevant point here is the randomization procedure for animal allocation into groups. On this occasion, the randomization process resulted in differences in lesion severity between groups. A pseudorandom allocation would have helped avoid this situation.

Taken together, our findings demonstrated that co-transplantation of NSCs with OECs can promote vascular and/or tissue remodeling in the ischemic brain as a result of synergistic

effects of the two cell types. Clearly, this was contingent on the extent of lesion severity. However, an important finding in our study was the evidence of OEC effects on *in situ* remodeling in more severe ischemic lesions, which seems to be in agreement with the pathway hypothesis. Notwithstanding that the variability of lesion pathology between subjects in a given cohort post-MCAo may confound a thorough elucidation of the exact mechanisms involved, it is worth considering how future strategies for stroke repair may involve OECs as part of an *in situ* tissue engineering paradigm as an alternative to or in combination with other approaches, as for example tailored biomaterials [6, 7, 53, 55]. Such approaches, which incorporate state-of-the-art advances in the field [56] are highly promising with a view to preserving and/or restoring host tissue as well as optimizing implant-derived effects that enhance brain plasticity for functional restoration [6, 56].

Ethical approval

All applicable international, national, and/or institutional guidelines for the care and use of animals were followed. All procedures performed in studies involving animals were approved by the Norwegian ethics committee and were conducted in accordance with the relevant national, regional and site guidelines.

References

1. Doyle KP, Simon RP, Stenzel-Poore MP (2008) Mechanisms of ischemic brain damage. Neuropharmacology 55:310-318
2. Eltzschig HK, Eckle T (2011) Ischemia and reperfusion--from mechanism to translation. Nat Med 17:1391-1401
3. Fisher M (2004) The ischemic penumbra: identification, evolution and treatment concepts. Cerebrovasc Dis 17 Suppl 1:1-6
4. Robinson T, Zaheer Z, Mistri AK (2011) Thrombolysis in acute ischaemic stroke: an update. Therapeutic advances in chronic disease 2:119-131
5. Chen L, Qiu R, Li L, He D, Lv H, Wu X, Gu N (2014) The role of exogenous neural stem cells transplantation in cerebral ischemic stroke. Journal of biomedical nanotechnology 10:3219-3230
6. Jendelova P, Kubinova S, Sandvig I, Erceg S, Sandvig A, Sykova E (2016) Current developments in cell- and biomaterial-based approaches for stroke repair. Expert opinion on biological therapy 16:43-56
7. Bible E, Qutachi O, Chau DY, Alexander MR, Shakesheff KM, Modo M (2012) Neo-vascularization of the stroke cavity by implantation of human neural stem cells on VEGF-releasing PLGA microparticles. Biomaterials 33:7435-7446
8. Patkar S, Tate R, Modo M, Plevin R, Carswell HV (2012) Conditionally immortalised neural stem cells promote functional recovery and brain plasticity after transient focal cerebral ischaemia in mice. Stem cell research 8:14-25
9. Smith EJ, Stroemer RP, Gorenkova N, Nakajima M, Crum WR, Tang E, Stevanato L, Sinden JD, Modo M (2012) Implantation site and lesion topology determine efficacy of a human neural stem cell line in a rat model of chronic stroke. Stem cells (Dayton, Ohio) 30:785-796
10. De Feo D, Merlini A, Laterza C, Martino G (2012) Neural stem cell transplantation in central nervous system disorders: from cell replacement to neuroprotection. Current opinion in neurology 25:322-333
11. Kokaia Z, Martino G, Schwartz M, Lindvall O (2012) Cross-talk between neural stem cells and immune cells: the key to better brain repair? Nature neuroscience 15:1078-1087
12. Andres RH, Choi R, Steinberg GK, Guzman R (2008) Potential of adult neural stem cells in stroke therapy. Regenerative medicine 3:893-905
13. Franklin RJ, Barnett SC (2000) Olfactory ensheathing cells and CNS regeneration: the sweet smell of success? Neuron 28:15-18
14. Dai C, Khaw PT, Yin ZQ, Li D, Raisman G, Li Y (2012) Olfactory Ensheathing Cells Rescue Optic Nerve Fibers in a Rat Glaucoma Model. Translational vision science & technology 1:3
15. Li J, Chen W, Li Y, Chen Y, Ding Z, Yang D, Zhang X (2015) Transplantation of olfactory ensheathing cells promotes partial recovery in rats with experimental autoimmune encephalomyelitis. International journal of clinical and experimental pathology 8:11149-11156

16. Li Y, Li D, Raisman G (2016) Functional Repair of Rat Corticospinal Tract Lesions Does Not Require Permanent Survival of an Immunoincompatible Transplant. Cell transplantation 25:293-299
17. Toft A, Scott DT, Barnett SC, Riddell JS (2007) Electrophysiological evidence that olfactory cell transplants improve function after spinal cord injury. Brain : a journal of neurology 130:970-984
18. Toft A, Tome M, Lindsay SL, Barnett SC, Riddell JS (2012) Transplant-mediated repair properties of rat olfactory mucosal OM-I and OM-II sphere-forming cells. Journal of neuroscience research 90:619-631
19. Sandvig I, Thuen M, Hoang L, Olsen O, Sardella TC, Brekken C, Tvedt KE, Barnett SC, Haraldseth O, Berry M, Sandvig A (2012) In vivo MRI of olfactory ensheathing cell grafts and regenerating axons in transplant mediated repair of the adult rat optic nerve. NMR in biomedicine 25:620-631
20. Lakatos A, Franklin RJ, Barnett SC (2000) Olfactory ensheathing cells and Schwann cells differ in their in vitro interactions with astrocytes. Glia 32:214-225
21. Lakatos A, Barnett SC, Franklin RJ (2003) Olfactory ensheathing cells induce less host astrocyte response and chondroitin sulphate proteoglycan expression than Schwann cells following transplantation into adult CNS white matter. Exp Neurol 184:237-246
22. Tabakow P, Raisman G, Fortuna W, Czyz M, Huber J, Li D, Szewczyk P, Okurowski S, Miedzybrodzki R, Czapiga B, Salomon B, Halon A, Li Y, Lipiec J, Kulczyk A, Jarmundowicz W (2014) Functional regeneration of supraspinal connections in a patient with transected spinal cord following transplantation of bulbar olfactory ensheathing cells with peripheral nerve bridging. Cell transplantation 23:1631-1655
23. Li Y, Carlstedt T, Berthold CH, Raisman G (2004) Interaction of transplanted olfactory-ensheathing cells and host astrocytic processes provides a bridge for axons to regenerate across the dorsal root entry zone. Experimental neurology 188:300-308
24. Chuah MI, Hale DM, West AK (2011) Interaction of olfactory ensheathing cells with other cell types in vitro and after transplantation: glial scars and inflammation. Experimental neurology 229:46-53
25. Memezawa H, Smith ML, Siesjo BK (1992) Penumbral tissues salvaged by reperfusion following middle cerebral artery occlusion in rats. Stroke 23:552-559
26. Haberg A, Qu H, Haraldseth O, Unsgard G, Sonnewald U (1998) In vivo injection of [1-13C]glucose and [1,2-13C]acetate combined with ex vivo 13C nuclear magnetic resonance spectroscopy: a novel approach to the study of middle cerebral artery occlusion in the rat. J Cereb Blood Flow Metab 18:1223-1232
27. Modo M, Rezaie P, Heuschling P, Patel S, Male DK, Hodges H (2002) Transplantation of neural stem cells in a rat model of stroke: assessment of short-term graft survival and acute host immunological response. Brain Res 958:70-82

28. Feigin VL, Barker-Collo S, Krishnamurthi R, Theadom A, Starkey N (2010) Epidemiology of ischaemic stroke and traumatic brain injury. Best practice & research Clinical anaesthesiology 24:485-494
29. Liu SJ, Zou Y, Belegu V, Lv LY, Lin N, Wang TY, McDonald JW, Zhou X, Xia QJ, Wang TH (2014) Co-grafting of neural stem cells with olfactory en sheathing cells promotes neuronal restoration in traumatic brain injury with an anti-inflammatory mechanism. Journal of neuroinflammation 11:66
30. Shukla S, Chaturvedi RK, Seth K, Roy NS, Agrawal AK (2009) Enhanced survival and function of neural stem cells-derived dopaminergic neurons under influence of olfactory ensheathing cells in parkinsonian rats. Journal of neurochemistry 109:436-451
31. Li Y, Li D, Raisman G (2005) Interaction of olfactory ensheathing cells with astrocytes may be the key to repair of tract injuries in the spinal cord: the 'pathway hypothesis'. Journal of neurocytology 34:343-351
32. Ao Q, Wang AJ, Chen GQ, Wang SJ, Zuo HC, Zhang XF (2007) Combined transplantation of neural stem cells and olfactory ensheathing cells for the repair of spinal cord injuries. Medical hypotheses 69:1234-1237
33. Wang G, Ao Q, Gong K, Zuo H, Gong Y, Zhang X (2010) Synergistic effect of neural stem cells and olfactory ensheathing cells on repair of adult rat spinal cord injury. Cell transplantation 19:1325-1337
34. Coralli C, Cemazar M, Kanthou C, Tozer GM, Dachs GU (2001) Limitations of the reporter green fluorescent protein under simulated tumor conditions. Cancer Res 61:4784-4790
35. Heim R, Prasher DC, Tsien RY (1994) Wavelength mutations and posttranslational autoxidation of green fluorescent protein. Proc Natl Acad Sci U S A 91:12501-12504
36. Modo M, Cash D, Mellodew K, Williams SC, Fraser SE, Meade TJ, Price J, Hodges H (2002) Tracking transplanted stem cell migration using bifunctional, contrast agent-enhanced, magnetic resonance imaging. Neuroimage 17:803-811
37. Modo M, Mellodew K, Cash D, Fraser SE, Meade TJ, Price J, Williams SC (2004) Mapping transplanted stem cell migration after a stroke: a serial, in vivo magnetic resonance imaging study. Neuroimage 21:311-317
38. Zhu WZ, Li X, Qi JP, Tang ZP, Wang W, Wei L, Lei H (2008) Experimental study of cell migration and functional differentiation of transplanted neural stem cells co-labeled with superparamagnetic iron oxide and BrdU in an ischemic rat model. Biomed Environ Sci 21:420-424
39. Lu P, Jones LL, Snyder EY, Tuszynski MH (2003) Neural stem cells constitutively secrete neurotrophic factors and promote extensive host axonal growth after spinal cord injury. Experimental neurology 181:115-129
40. Barnett SC, Riddell JS (2007) Olfactory ensheathing cell transplantation as a strategy for spinal cord repair--what can it achieve? Nature clinical practice Neurology 3:152-161

41. Barnett SC, Riddell JS (2004) Olfactory ensheathing cells (OECs) and the treatment of CNS injury: advantages and possible caveats. J Anat 204:57-67
42. Ding DC, Lin CH, Shyu WC, Lin SZ (2013) Neural stem cells and stroke. Cell Transplant 22:619-630
43. Jackson JS, Golding JP, Chapon C, Jones WA, Bhakoo KK (2010) Homing of stem cells to sites of inflammatory brain injury after intracerebral and intravenous administration: a longitudinal imaging study. Stem cell research & therapy 1:17
44. Guzman R, Uchida N, Bliss TM, He D, Christopherson KK, Stellwagen D, Capela A, Greve J, Malenka RC, Moseley ME, Palmer TD, Steinberg GK (2007) Long-term monitoring of transplanted human neural stem cells in developmental and pathological contexts with MRI. Proc Natl Acad Sci U S A 104:10211-10216
45. Nudo RJ (2007) Postinfarct cortical plasticity and behavioral recovery. Stroke 38:840-845
46. Reglodi D, Tamas A, Lengvari I (2003) Examination of sensorimotor performance following middle cerebral artery occlusion in rats. Brain Res Bull 59:459-466
47. Schallert T, Fleming SM, Leasure JL, Tillerson JL, Bland ST (2000) CNS plasticity and assessment of forelimb sensorimotor outcome in unilateral rat models of stroke, cortical ablation, parkinsonism and spinal cord injury. Neuropharmacology 39:777-787
48. Schaar KL, Brenneman MM, Savitz SI (2010) Functional assessments in the rodent stroke model. Experimental & translational stroke medicine 2:13
49. Doeppner TR, Kaltwasser B, Teli MK, Sanchez-Mendoza EH, Kilic E, Bahr M, Hermann DM (2015) Post-stroke transplantation of adult subventricular zone derived neural progenitor cells--A comprehensive analysis of cell delivery routes and their underlying mechanisms. Exp Neurol 273:45-56
50. Mine Y, Tatarishvili J, Oki K, Monni E, Kokaia Z, Lindvall O (2013) Grafted human neural stem cells enhance several steps of endogenous neurogenesis and improve behavioral recovery after middle cerebral artery occlusion in rats. Neurobiol Dis 52:191-203
51. Fluri F, Schuhmann MK, Kleinschnitz C (2015) Animal models of ischemic stroke and their application in clinical research. Drug design, development and therapy 9:3445-3454
52. Howells DW, Porritt MJ, Rewell SS, O'Collins V, Sena ES, van der Worp HB, Traystman RJ, Macleod MR (2010) Different strokes for different folks: the rich diversity of animal models of focal cerebral ischemia. J Cereb Blood Flow Metab 30:1412-1431
53. Massensini AR, Ghuman H, Saldin LT, Medberry CJ, Keane TJ, Nicholls FJ, Velankar SS, Badylak SF, Modo M (2015) Concentration-dependent rheological properties of ECM hydrogel for intracerebral delivery to a stroke cavity. Acta biomaterialia 27:116-130
54. Kazanis I, Gorenkova N, Zhao JW, Franklin RJ, Modo M, Ffrench-Constant C (2013) The late response of rat subependymal zone stem and progenitor cells to stroke is restricted to directly affected areas of their niche. Exp Neurol 248:387-397

55. Sandvig I, Karstensen K, Rokstad AM, Aachmann FL, Formo K, Sandvig A, Skjak-Braek G, Strand BL (2014) RGD-peptide modified alginate by a chemoenzymatic strategy for tissue engineering applications. Journal of biomedical materials research Part A
56. Janowski M, Wagner DC, Boltze J (2015) Stem Cell-Based Tissue Replacement After Stroke: Factual Necessity or Notorious Fiction? Stroke 46:2354-2363